Supplement of Atmos. Chem. Phys., 14, 10705–10719, 2014
http://www.atmos-chem-phys.net/14/10705/2014/
doi:10.5194/acp-14-10705-2014-supplement

Atmospheric Chemistry and Physics Open Access

Supplement of

Estimating regional greenhouse gas fluxes: an uncertainty analysis of planetary boundary layer techniques and bottom-up inventories

X. Zhang et al.

Correspondence to: X. Zhang (zhangxin.yale@gmail.com)

Supplementary materials

S1 The storage term in the tall-tower eddy covariance method

The storage term (F_S) for the tall tower EC method was calculated as the aggregated CO_2 concentration change over time from the land surface to the height of EC measurement (Davis et al., 2003)

$$\mathrm{F_S} = \int_0^{z_r} \frac{\partial \bar{c}}{\partial t} dz$$

In this equation, z_r is the height of the EC measurement (100 m at the KCMP tower), $\frac{\partial \bar{c}}{\partial t}$ is the change of CO_2 mixing ratio over time. CO_2 mixing ratios were measured sequentially at the 32 m, 56 m, 100 m, and 200 m heights during the EC measurement. The storage term was calculated by interpolating the four-layer measurement to a concentration profile from land surface (0 m) to 200 m, assuming the concentration in 0-32 m layer the same as the concentration measured at 32 m.

The storage term is often negative in early morning due to the fast CO_2 depletion in the boundary layer during its transition from stable to turbulent conditions (Anthoni et al., 1999; Davis et al., 2003; Yi et al., 2000). The absolute value of the storage term is especially large after calm night, which could not be explained by environmental variables.

To avoid the uncertainties caused by including the irregularly large morning uptake flux, several studies have screened the flux data by setting a threshold for the storage term for morning hours. For example, Anthoni et al. (1999) replace the EC flux measured at 46 m with modeled value when the storage term were more negative than -2 μmol m^{-2} s^{-1}.

We tested four screening standards for the negative storage term in the morning: no removal, and removal of the CO_2 flux data when the storage term is lower than -6 μmol m^{-2} s^{-1}, -4 μmol m^{-2} s^{-1}, -2 μmol m^{-2} s^{-1}, respectively. The result suggests that removing morning CO_2 flux data with large storage term reduces the overestimation of CO_2 uptake in the month of July, August, and September (Figure S1). The higher the standard is (from -6 μmol m^{-2} s^{-1} to -2 μmol m^{-2} s^{-1}), the smaller the monthly CO_2 uptake is. The result from the standard of -6 μmol m^{-2} s^{-1} and -4 μmol m^{-2} s^{-1} are similar, while the result from the standard of -2 μmol m^{-2} s^{-1} has much smaller uptake in August. The more stringent screening standard (-2 μmol m^{-2} s^{-1}) left less than 20% data available for the period of 8 a.m.-10 a.m., therefore, the CO_2 fluxes during this period were all positive, despite that CO_2 fluxes from major land cover types around the tall tower were negative (Figure S2c). In contrast, the diurnal pattern of CO_2 flux using -4 μmol m^{-2} s^{-1} as the screening standard has better agreement with CO_2 fluxes from major land cover types around the tall tower (Figure S2b).

In addition, the -4 μmol m^{-2} s^{-1} screening standard reduced the estimated CO_2 uptake during the growing season (May to September) by 18% and is consistent with that reported in the literature (Davis et al., 2003; Yi et al., 2000).

Therefore, in this study, we removed the morning (06:00 and 10:00 LST) data when the storage term was lower than -4 μmol m^{-2} s^{-1}.

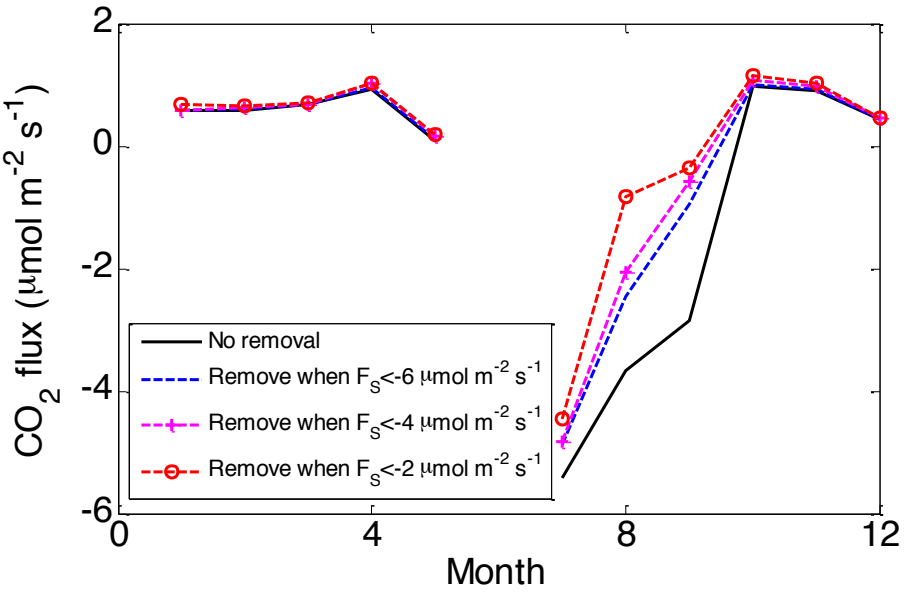

Figure S1 Monthly averaged CO_2 flux using different data screening standard for the storage term (Fs)

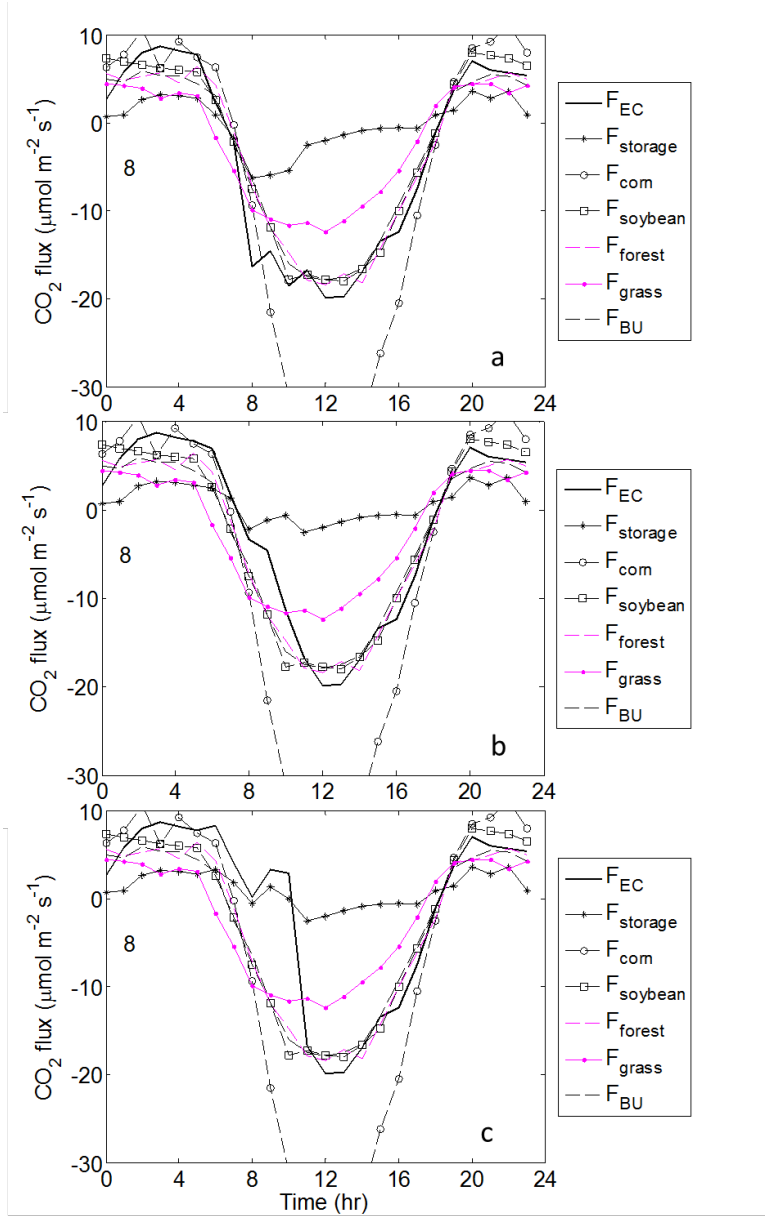

Figure S2 The diurnal composite of CO_2 flux for August with different screening standard for the storage term in the morning: a) no removal; b) remove when the storage term lower than -4 μmol m^{-2} s^{-1} ; c) remove when the storage term lower than -2 μmol m^{-2} s^{-1}. F_{EC} is the CO_2 flux determined by the tall tower EC measurement; $F_{storage}$ is the storage term for F_{EC}; F_{corn} , $F_{soybean}$, F_{grass} are the CO_2 fluxes measured by EC in corn field, soybean field, and grassland respectively; F_{BU} is the CO_2 fluxes estimated using flux aggregation method.

S2 "Diurnal composite" method for calculating the monthly flux and the uncertainty range

We estimated the monthly flux from the hourly fluxes using a "diurnal composite" method with the following steps:

1. Compute an averaged diurnal cycle for a month by averaging all of the available data within each hour (from 0:00 to 23:00).
2. The monthly mean flux, therefore, represents the average of the diurnal composite. Further, the annual flux represents the average of the monthly fluxes.

Therefore, when no data gap exists, the monthly value from the "diurnal composite" method is the same as the monthly mean of the all available data within the month. To evaluate the uncertainty associated with data gaps, we performed a Monte Carlo simulation following Griffis et al. (2003): We randomly removed 30% of the data for each month, and recorded the calculated monthly and annual fluxes following the same data processing procedure described above. By repeating this simulation 5000 times, we determined the standard deviation of the annual flux estimates.

S3 The footprint map

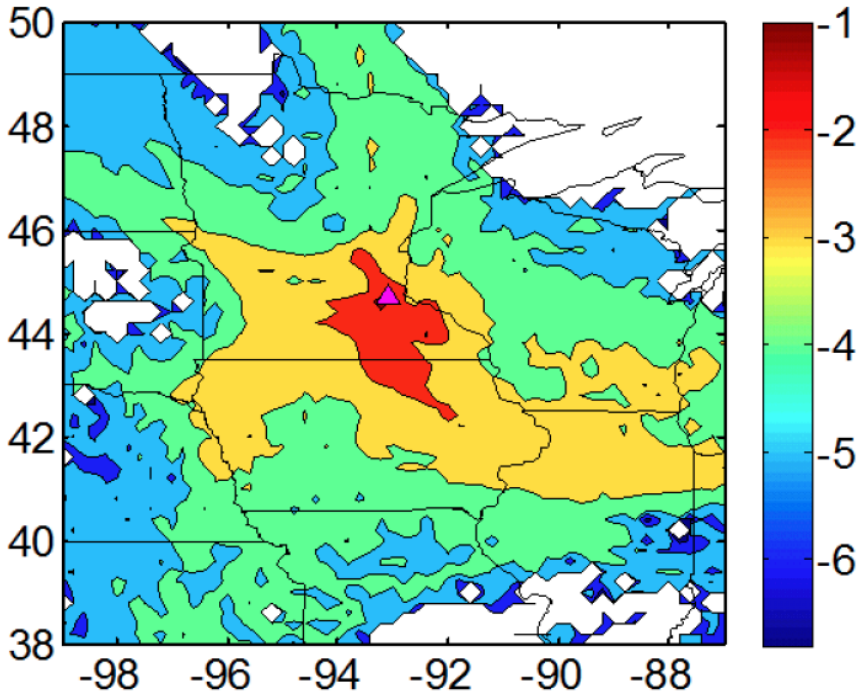

Figure S3. Concentration footprint of the tall tower determined using the STILT model in September 2009. The color scale represents the log10 footprint, and the unit of the footprint is ppm (μmole m^{-2} s^{-1})$^{-1}$

S4 Uncertainties in the EQ method due to free tropospheric CO_2

Using the CO_2 mixing ratio at the NWR site as the approximation of the CO_2 mixing ratio in the free troposphere is one of the uncertainty sources for the EQ method. To evaluate such uncertainties, we first compared the CO_2 mixing ratio at the NWR site with the Marine Boundary Layer (MBL) CO_2 at the latitude of 44°N and aircraft measurements at three aircraft measurement sites close to the KCMP tower (Figure S4); then we use those mixing ratios as the free tropospheric CO_2 (c+) at the KCMP site to calculate the CO_2 flux with the EQ method (Figure S5). The three aircraft measurement sites include LEF (Park Falls, Wisconsin, 45.9451°N, 90.2732 °W), WBI (West Branch, Iowa, 41.7248 °N, 91.3529 °W), and DND (Dahlen, North Dakota, 47.5000 °N, 99.2400 °W). Those are the closest sites to KCMP with available aircraft measurements in 2009 (Cooperative Global Atmospheric Data Integration Project, 2014).

The aircraft measurements at the three sites near KCMP shows similar seasonal pattern as the CO_2 mixing ratio at the NWR site. The CO_2 mixing ratio in the MBL at the same latitude as the KCMP tower is significantly lower than NWR site and the three aircraft measurement sites from July to September. Therefore, using the MBL as the free tropospheric CO_2 (c+) at the KCMP site produces lower estimates of the CO_2 uptake in this period. In contrast, using different data sources for c+ does not make significant difference in CO_2 flux from October to April.

Given ρW from equation 3, the annual CO_2 budget estimates range from 13 to 58 g C-CO_2 m^{-2} yr^{-1} due to using different data sources for c+; while the estimates range from 46 to 105 g C-CO_2 m^{-2} yr^{-1}, given ρW from equation 4 (Table S1). In both cases, the estimates using the CO_2 mixing ratio at the NWR site locate in the middle of the range.

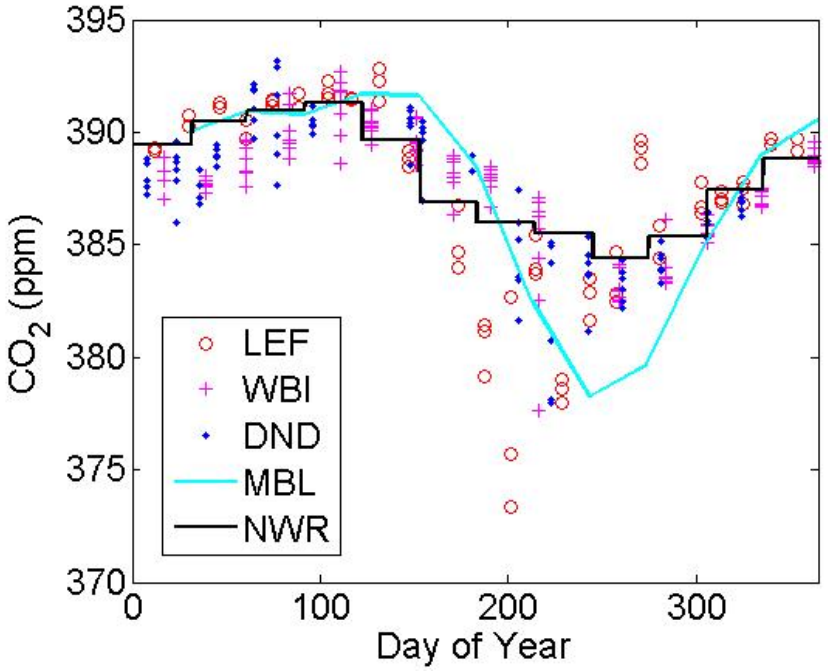

Figure S4 A summary of the CO_2 mixing ratio at three aircraft measurement sites (LEF, WBI, and DND), one background site (NWR), and the latitude of 44°N in Marin Boundary Layer in 2009 (Cooperative Global Atmospheric Data Integration Project, 2014). No aircraft measurement was available at the KCMP site. The aircraft measurement was conducted about two times a month from about 4000m to 500 m, but we only shows the measurements above 3000m in this figure.

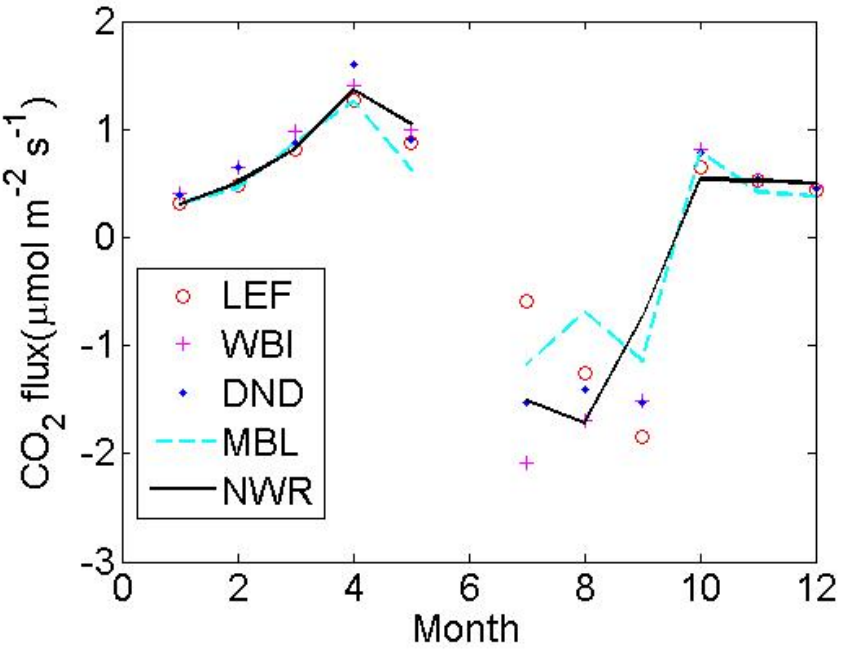

Figure S5 Monthly CO_2 flux calculated using EQ method with different approximation of free tropospheric CO_2 (c+) and ρW from equation 3.

Table S1 An summary of annual CO_2 flux using different approximation of free tropospheric CO_2 (c+) and ρW from two methods.

Data source for c+	**Annual CO_2 flux (g C-CO_2 m^{-2} yr^{-1})**	
	Use ρW from equation 3	Use ρW from equation 4
LEF	58	105
WBI	13	46
DND	46	94
MBL	58	103
NWR	46	74

S5 ρW calculated from different approaches

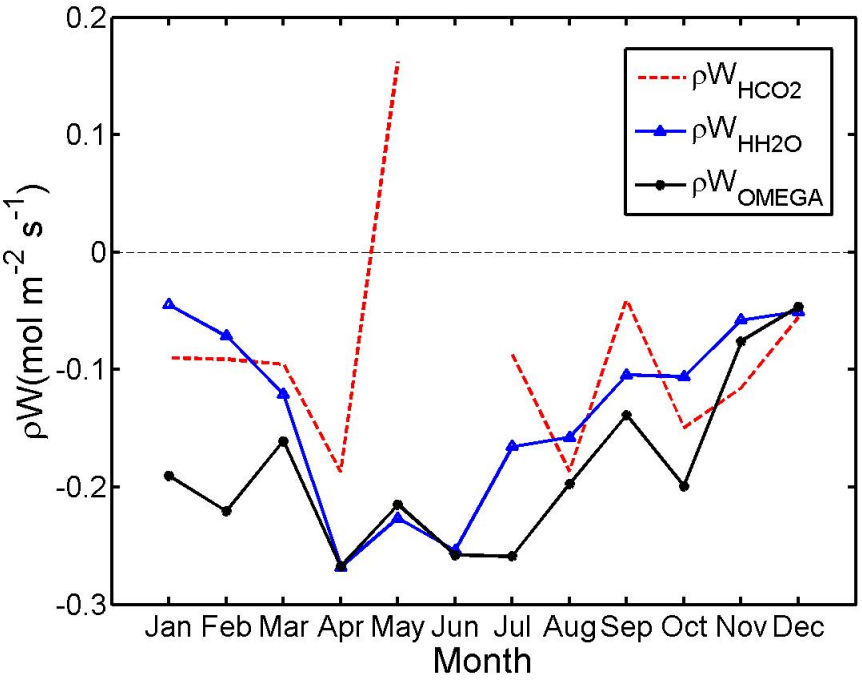

Figure S6 Monthly ρW calculated from different method. ρW_{HH2O}, ρW_{OMEGA}, and ρW_{HCO2} were calculated from equation 3,4,5 respectively.

S6 A comparison with the EPA GHG inventory

The EPA inventory was developed according to the IPCC guidelines with more country-specific emission factors or models (US EPA, 2014); for example, the N_2O emission from agriculture soil was determined using the DAYCENT model (Del Grosso et al., 2010), a Tier 3 approach. However, because the inventory is mostly organized by sectors, not by spatial distribution, it is difficult to make a direct comparison between the EPA inventory and our top-down estimates for the Upper Midwest US region. Nevertheless, we compared the annual emission of the three major GHGs (CO_2, CH_4 and N_2O) from the US in 2009 (Table S2). The result indicates that

1) The EPA inventory was only 4% higher than the EDGAR inventory for the CO_2 emission from the Energy and Industrial Processes categories. We only compare the Energy and Industrial Processes categories since we only used those categories in our comparison for top-down and bottom-up methods for CO_2.
2) The EPA inventory was 12% and 35% higher than the EDGAR inventory for CH_4 and N_2O emissions, respectively. The major difference for CH_4 emission was in fugitive emissions from oil and national gas (in the Energy category), while the major difference for N_2O was in agricultural soils (in the Agriculture category).

If the EPA inventory has a similar spatial distribution as the EDGAR inventory in the US, a comparison between the bottom-up inventory and the top-down flux estimates can be carried out. The result was similar to the comparison using the EDGAR inventory: the EPA inventory 1) was in good agreement with top-down estimates for CO_2 flux; 2) it underestimated the CH_4 flux by 5-8 times (as compared to 6-9 times for EDGAR inventory); 3) it underestimated the N_2O flux by 1-2 times (2-3 for EDGAR inventory).

A better assessment of the EPA inventory with the top-down flux will require more information on the spatial distribution of the EPA inventory.

Table S2 A comparison of annual GHG emission in 2009 between EPA GHG inventory[1] and EDGAR[2]

GREENHOUSE GAS SOURCE AND SINK CATEGORIES	**CO_2 (Gg)**		**CH_4 (Gg)**		**N_2O (Gg)**	
	EPA	**EDGAR**	**EPA**	**EDGAR**	**EPA**	**EDGAR**
1. Energy	5378059	5167519	12037	10175	141	200
2. Industrial Processes	119745	131836	156	24	54	72
3. Solvent and Other Product Use	NA	6195	0	0	14	17
4. Agriculture	0	12001	9749	9303	1078	585
5. Land Use, Land-Use Change and Forestry	-953306	43738	275	48	21	3
6. Waste	NA	0	6190	5678	21	35
7. Other	NA	4730	NA	15	NA	70
Total	**4544498**	**5366018**	**28406**	**25242**	**1330**	**983**

[1] The data for the EPA inventory was downloaded from http://www.epa.gov/climatechange/ghgemissions/usinventoryreport.html

[2] The data for the EDGAR inventory was downloaded from http://edgar.jrc.ec.europa.eu/

S7 The fraction of six major land cover types in different tall tower footprints

Table S3 A summary of the fraction of major land cover types ($frac_i$) in different tall tower footprints

Land cover type	**Equally-weighted circular footprint**								**STILT footprint (Sep., 2009)**
(radius)	5 km	10 km	20 km	50 km	100 km	200 km	300 km	600 km	NA
Cropland	48%	41%	39%	26%	36%	40%	39%	39%	65%
Forest	9%	9%	11%	17%	17%	24%	27%	20%	11%
Grassland	35%	30%	23%	24%	25%	19%	16%	22%	11%
Wetland	1%	1%	1%	3%	4%	5%	7%	7%	2%
Open water	0%	1%	4%	4%	4%	3%	3%	3%	4%
Developed land	7%	19%	22%	26%	14%	9%	8%	8%	6%

Reference

Anthoni, P. M., Law, B. E., and Unsworth, M. H.: Carbon and water vapor exchange of an open-canopied ponderosa pine ecosystem, Agric. For. Meteorol., 95, 151-168, doi:10.1016/s0168-1923(99)00029-5, 1999.

Cooperative Global Atmospheric Data Integration Project: Multi- laboratory compilation of atmospheric carbon dioxide data for the period 2000-2013 (obspack_co2_1_CARBONTRACKER_CT2013_2014-05-08). Compiled by NOAA Global Monitoring Division: Boulder, Colorado, U.S.A. Data product accessed at http://www.esrl.noaa.gov/gmd/ccgg/obspack/, 2014.

Davis, K. J., Bakwin, P. S., Yi, C. X., Berger, B. W., Zhao, C. L., Teclaw, R. M., and Isebrands, J. G.: The annual cycles of CO_2 and H_2O exchange over a northern mixed forest as observed from a very tall tower, Global Change Biol, 9, 1278-1293, doi:10.1046/j.1365-2486.2003.00672.x, 2003.

Del Grosso, S., Ogle, S., Parton, W., and Breidt, F.: Estimating uncertainty in N_2O emissions from US cropland soils, Global Biogeochemical Cycles, 24, (1), 2010.

Griffis, T. J., Black, T. A., Morgenstern, K., Barr, A. G., Nesic, Z., Drewitt, G. B., Gaumont-Guay, D., and McCaughey, J. H.: Ecophysiological controls on the carbon balances of three southern boreal forests, Agric. For. Meteorol., 117, 53-71, doi:10.1016/s0168-1923(03)00023-6, 2003.

U.S. EPA: Inventory of U.S. Greenhouse Gas Emissions and Sinks: 1990–2012, 529 pp., Washington, D.C., 2014.

Yi, C., Davis, K. J., Bakwin, P. S., Berger, B. W., and Marr, L. C.: Influence of advection on measurements of the net ecosystem-atmosphere exchange of CO_2 from a very tall tower, Journal of Geophysical Research-Atmospheres, 105, 9991-9999, doi:10.1029/2000jd900080, 2000.